Case Study of Condensate Dropout Effect in Unconventional Gas/Condensate Reservoirs with Hydraulically Fractured Wells

Alsultan, Ali H.; Shaoul, Josef R.; Park, Jason; Zitha, Pacelli L.J.

DOI
10.2118/205252-MS

Publication date
2022

Document Version
Final published version

Published in
Society of Petroleum Engineers - SPE International Hydraulic Fracturing Technology Conference and Exhibition, IHFT 2022

SPE-205252-MS

Case Study of Condensate Dropout Effect in Unconventional Gas/Condensate Reservoirs with Hydraulically Fractured Wells

Ali H. Alsultan, Saudi-Aramco, Delft University of Technology; Josef R. Shaoul and Jason Park, Fenix Consulting Delft; Pacelli L. J. Zitha, Delft University of Technology

This paper was prepared for presentation at the SPE International Hydraulic Fracturing Technology Conference & Exhibition, Muscat, Oman, 11 - 13 January 2022.

Abstract

Condensate banking is a major issue in the production operations of gas condensate reservoirs. Increase in liquid saturation in the near-wellbore zone due to pressure decline below dew point, decreases well deliverability and the produced condensate-gas ratio (CGR). This paper investigates the effects of condensate banking on the deliverability of hydraulically fractured wells producing from ultralow permeability (0.001 to 0.1 mD) gas condensate reservoirs. Cases where condensate dropout occurs over a large volume of the reservoir, not only near the fracture face, were examined by a detailed numerical reservoir simulation.

A commercial compositional simulator with local grid refinement (LGR) around the fracture was used to quantify condensate dropout as a result of reservoir pressure decline and its impact on well productivity index (PI). The effects of gas production rate and reservoir permeability were investigated. Numerical simulation results showed a significant change in fluid compositions and relative permeability to gas over a large reservoir volume due to pressure decline during reservoir depletion. Results further illustrated the complications in understanding the PI evolution of hydraulically fractured wells in "unconventional" gas condensate reservoirs and illustrate how to correctly evaluate fracture performance in such a situation.

The findings of our study and novel approach help to more accurately predict post-fracture performance. They provide a better understanding of the hydrocarbon phase change not only near the wellbore and fracture, but also deep in the reservoir, which is critical in unconventional gas condensate reservoirs. The optimization of both fracture spacing in horizontal wells and well spacing for vertical well developments can be achieved by improving the ability of production engineers to generate more realistic predictions of gas and condensate production over time.

Introduction

The production of hydrocarbons from retrograde gas condensate reservoirs often suffers from severe productivity decline due to condensate drop-out. As reservoir pressure decreases below dewpoint pressure, liquid accumulates in the near-wellbore zone, thus chocking the flow of gas towards the well. As a result,

both gas and condensate production decrease, and the gas produced at surface contains fewer more valuable heavy ends (Fan et al. 2005).

In the last decade, several reservoir-scale numerical simulation studies on condensate drop-out and the ensuing productivity decline have been reported in the literature. Bellow we provide a brief survey of the existing works with a particular emphasis on fractured reservoirs. Concepts for which there is consensus are developed and gaps in understanding are highlighted.

El-Banbi et al. (2000) used a compositional reservoir simulator to model and history-match the productivity of several wells drilled in a moderately rich gas-condensate reservoir. All wells showed a similar trend: first the productivity decreased rapidly and then it increased as the reservoir was depleted. The authors showed that during the early production, a ring of condensate was rapidly formed around each well once the pressure decreased below the dewpoint pressure. The condensate saturation in this ring was considerably higher than the maximum condensate dropout predicted by the static PVT laboratory work. The higher condensate saturation in the near-wellbore is due to the steeper decrease of the pressure due to the lowering of the gas relative permeability. A leaner gas was produced as increasing condensate drops out and is trapped around the well, resulting in gas productivity decrease for a long time (six years). At the end of this period, the condensate drop-out extended over an area with a radius of 100s meters from the well. Subsequently, the gas flowing into the condensate ring finally became leaner, causing the condensate saturation near the well to decrease, resulting in a gas productivity increase in the well. Barnum et al. (1995) reviewed data from 17 fields and showed that severe drop in gas recovery occurs due to near wellbore condensate banking, primarily in low productivity reservoirs, with a permeability-thickness (kh) below 1,000 mD-ft. Fevang and Whitson (1996) suggested an accurate method for modeling the deliverability of gas-condensate wells and studied the effect of gas-oil relative permeability. They showed that the gas-condensate well deliverability impairment by near wellbore condensate banking is dependent only on relative permeability ratios and it happens when the gas and oil relative permeability ratios (k_{rg}/k_{ro}) are in the range of 0.05-0.3.

Several studies investigated condensate drop-out in the presence of hydraulic fractures. Al-Hashim and Hashmi (2000) reported a reservoir simulation study of the effect of hydraulic fracturing in a layered rich gas-condensate reservoir. The reservoir consisted of five layers, with permeability ranging from 0.08 to 115 mD. Nearly 68% of the gas reserves were confined to the layers with the lowest permeabilities. The authors found that hydraulic fracturing improved the productivity of a gas-condensate reservoir by three folds over non-fractured wells. This implies that hydraulically fractured wells can maintain the same production rates at a much lower drawdown than un-fractured wells. In addition, the duration of gas production at pressures above dewpoint pressure can be extended considerably because there is a smaller drawdown and no near-wellbore pressure losses due to condensate banking.

Al Habsi et. al. (2019) conducted a combined reservoir simulation and history matching of well test data of vertical well drilled into Barik formation with permeability of 1.0 mD and initial condensate yield of 65 STB/MMscf. With the study, they could not investigate the obvious fracture face skin increase due to condensate banking even when the well was producing far below dewpoint pressure. As long as the history matched fracture properties, a long effective fracture length (1,250 ft) and a high fracture conductivity (5,500 mD-ft), are maintained, none of the pressure build-up responses are overwhelmingly impacted by condensate dropout.

The objective of this study is to investigate the initial fracture clean-up testing and long-term production behavior of a hydraulically fractured well drilled into an ultra-tight gas-condensate reservoir. High spatial and temporal resolution 3-D numerical simulations were performed using an industry standard reservoir simulation package for both a synthetic model and a real field case. A commercial fracture modeling package was used to analyze the fracture treatments in the well as well as to make simulation grids at the locations of the fractures with output that can be directly used in the reservoir simulator. This allows us to better

understand the effect of condensate drop-out in the fracture and in the matrix. In this study, the PVT data collected in the field has been history matched and incorporated in the numerical model. By modeling the fracture and the matrix with local grid refinement, it was possible to simulate the details of production performance in the reservoir including the condensate drop-out over the three-year production period.

Case history

Field description

Field A is in a gas prolific region in the Arabian Peninsula. The hydrocarbon bearing reservoir in the field is late Cambrian - early Ordovician and generally consists of fluvial sandstone with interbedded marine siltstone and claystone. They are at the depth greater than 4,000 m TVDSS with reservoir pressure of 7,400-8,200 psi and reservoir temperature of 135-145 °C. The target horizons in Field A are both very tight. The effective permeability to gas in the better zone ranges from 0.1 to 0.3 mD and in the poor zone from 0.01 to 0.10 mD. Condensate-gas ratio in the field is in the range of 70-100 STB/MMscf which is relatively higher than the neighboring fields. Hydraulic fracturing is required in the field to exploit the tight - unconventional reservoirs in an economically viable way.

Well data and stimulation history

A vertical production well (Well A-09) targeting a poor horizon in the South development region of the field, was selected for this study, for the following main reasons: (1) the availability of a complete data set, including initial well test and long-term production data and (2) the fact that the well was fractured and tested prior to field startup, i.e. at the original reservoir pressure, above the dewpoint pressure for the specific reservoir temperature. Hence, the initial clean-up flow and testing was done with less condensate around the well.

In Well A-09, two stages of fracturing had been conducted in October 2011. A summary of the fracture treatment and analysis is shown in Table 1. Stage#1 was about a three times larger treatment compared to Stage#2 regarding total proppant amounts, resulting in a bigger fracture in Stage#1. The estimated propped fracture half-length is 1,696 ft and 1,175 ft for Stage #1 and Stage #2 respectively. Dimensionless fracture conductivities (FcD) are in the ranges of 0.52-1.48 assuming typical poor fracture clean-up in such low permeability reservoirs. The fracture dimensions and proppant concentrations are presented in Figure 1. Although these two different fractures are probably not connecting up with each other, they are likely to be overlapping significantly and we can regard these fractures in a practical sense as shown in the figure as being dominated by Stage #1.

Table 1—Summary of fracture treatment and analysis in Well A-09.

Stage	Fracture Treatment		Fracture Analysis					
	Total Proppant (1000lbm)	Maximum Proppant Concentration (ppg)	Propped Frac Half-Length (ft)	Propped Frac Height (ft)	Average Propped Frac Width (inch)	Proppant Conc. (lb/ft²)	Contacted *kh* (mD-ft)	FcD @ 96% Damage
Stage #1	704	7.5	1696	157	0.14	1.7	6.6	0.52
Stage #2	243	7.5	1175	105	0.10	1.0	2.6	1.48

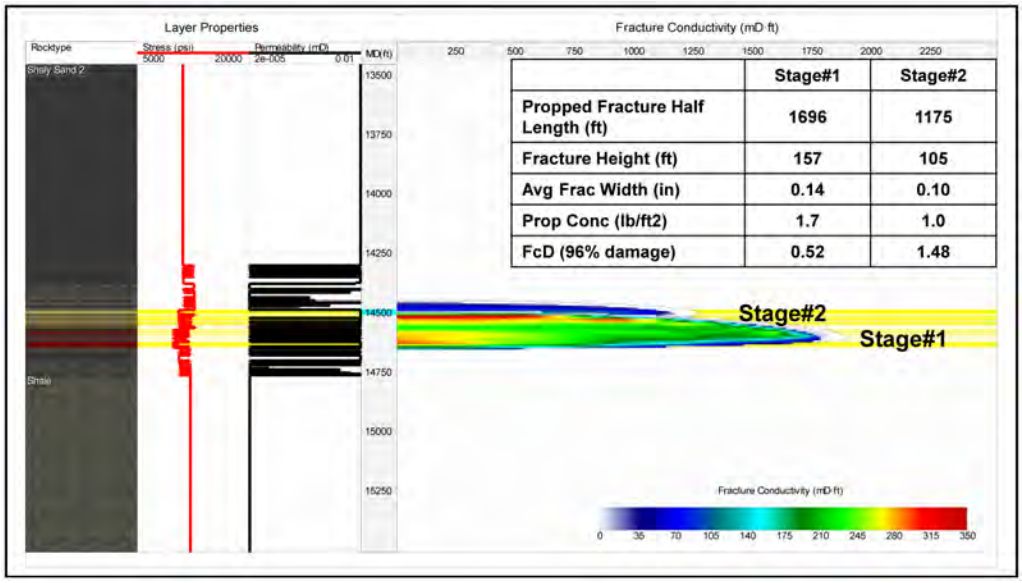

Figure 1—Fracture treatment result in A-09 Well.

Composition and PVT data

A downhole sample from a neighboring well producing from the same horizon was used for compositional and PVT analysis of the reservoir fluids. The composition of reservoir fluid is shown in Table 2, with all components heavier than lumped into the C12+ pseudo-component. A standard set of laboratory PVT tests for gas-condensate reservoir including dewpoint pressure measurement, constant composition expansion (CCE) and constant volume depletion (CVD) tests have been carried out. The theoretical maximum condensate-gas ratio by a single stage flash test was found to be 103 STB/MMscf. The laboratory analysis results were used to develop an equation of state (EOS) description of the fluid after matching both CVD and CCE with an industry standard PVT analysis software. Figure 2 shows very good matching of the CVD and the cumulative liquid production. The phase diagram obtained using the EOS is shown in Figure 3. At the reservoir temperature of 134 °C, the dewpoint pressure is 7,365 psi. Hence, the difference between the initial average reservoir pressure 7,470 psi and dewpoint pressure, also called headroom, is only 105 psi. Because of this rather small headroom and the very low reservoir permeability we expect the condensate to drop-out almost immediately after production begins.

Table 2—Composition of down-hole sample up to C12+.

Composition	Monophasic fluid	
	% Weight	% Mole
N_2	2.18	2.29
CO_2	1.64	1.10
H_2S	0.00	0.00
C1	42.31	77.56
C2	6.63	6.48
C3	4.36	2.91
IC4	1.43	0.72
NC4	2.19	1.11
IC5	1.16	0.47
NC5	1.37	0.56

Composition	Monophasic fluid	
	% Weight	% Mole
C6	2.88	1.01
C7	2.93	0.90
C8	3.09	0.85
C9	2.36	0.57
C10	2.60	0.57
C11	2.18	0.44
C12+	20.71	2.47
Total	100.00	100.00

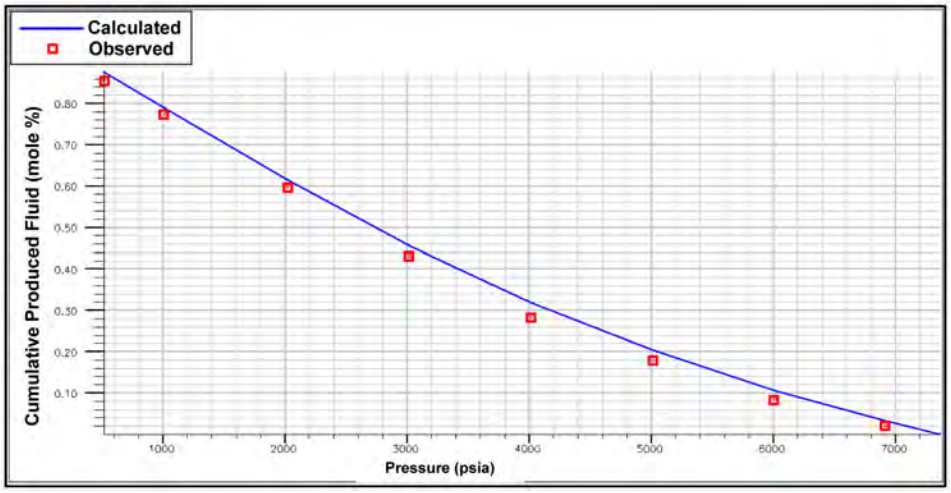

Figure 2—CVD matching results with down-hole sample.

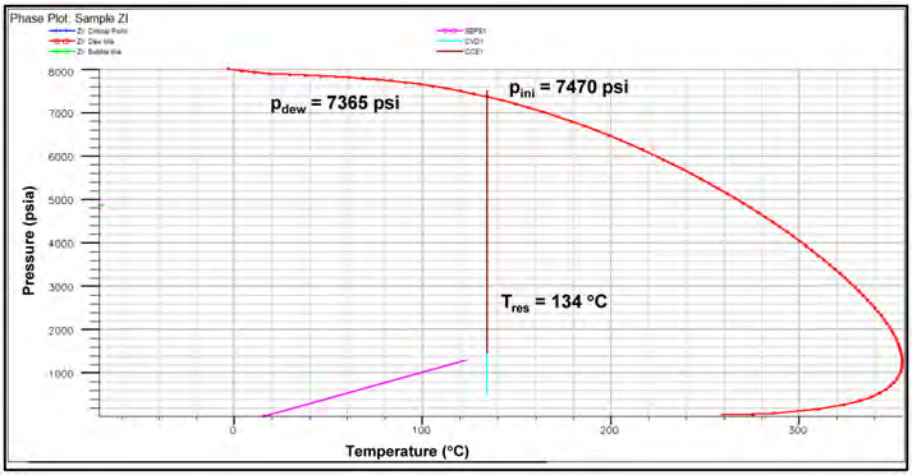

Figure 3—Phase diagram of the reservoir fluid.

Reservoir simulation model

A 3-D reservoir simulation model was built using commercial fracture modeling software. The advantage of the software is that it exports both the reservoir matrix and the history matched fracture properties in the formats of various commercial reservoir simulators. The fracture modeling tool uses a lumped 3-D fracture modeling technique developed by Crockett et.al. (1986). The grid generation as well as assigning

the petrophysical properties to the fracture is based on the work of Shaoul et.al. (2005). For this study we used an industry standard compositional reservoir simulator. The reservoir matrix and hydraulic fracture properties are exported to the reservoir simulator where they are used as the initial model parameters. A few parameters are then used as history-matching parameters, i.e. are varied until the reservoir simulations satisfactorily match the historical production data from the well.

The reservoir model is shown in Figure 4 and Figure 5. In Figure 4, the model with host grid only (above) and the model with host grid and local grid refinement (LGR) are compared. The model with host grid only is presented just for a comparison purpose with the model with LGR. As shown in the figure (Figure 4), it is a quarter symmetric model with the area of 506 ft × 1,600 ft, which is 3.24 million ft^2 (0.3 km^2) in term of full symmetry. Average water saturation is 0.25 and average porosity is 0.07 in the model. Water phase in tight matrix is assumed to be immobile with this low saturation. The initial reservoir pressure is 7,470 psi at the depth of 14,570 ft TVD. The initial gas in-place in terms of full symmetry is 8.2 Bcf.

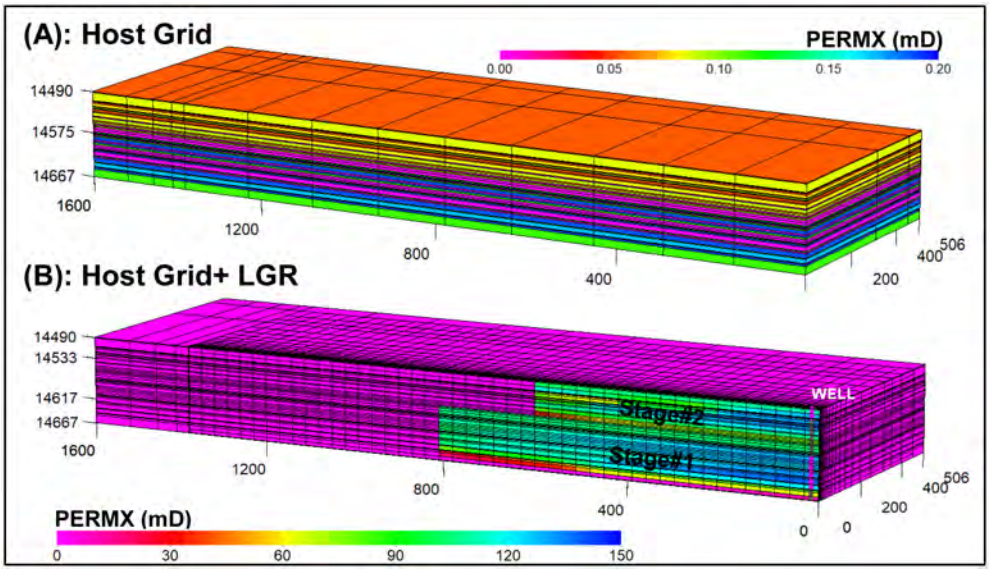

Figure 4—The 3-D reservoir simulation model (unit=ft): host grid only (above) and host grid with LGR (below).

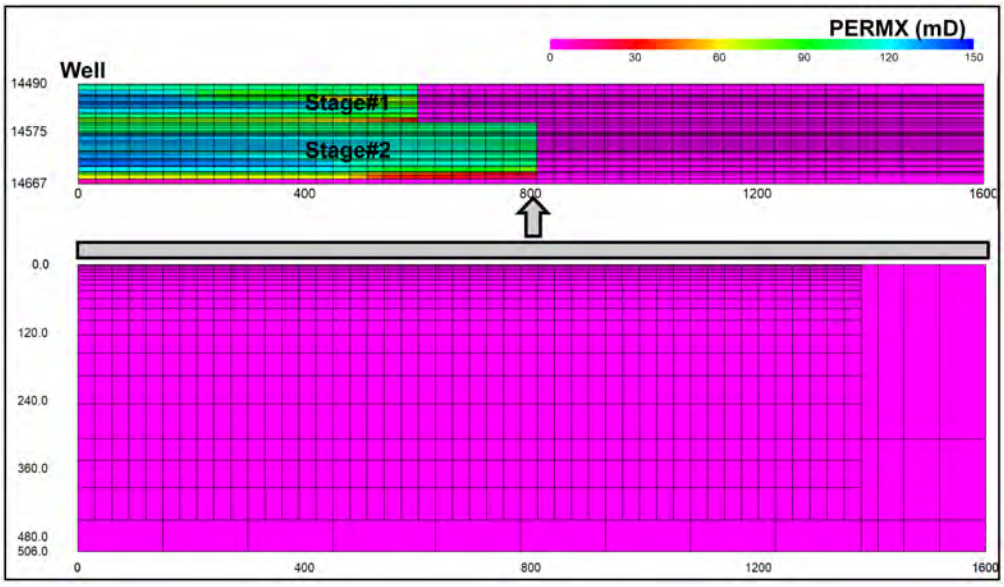

Figure 5—Details of the simulation model (unit=ft): a side view into the fracture (above) and a top view of the model (below).

The drainage of the well was determined by taking approximately one half of the inter-well distance, to limit the interference from neighboring wells. The effect of the hydraulic fracture on the reservoir stimulation is presented by the enhanced permeability in the LGR (Figure 5), which is obtained by upscaling the propped fracture width obtained from the fracture treatment analysis. The fracture width in the model is upscaled to 1 ft instead of the actual propped width of ~0.10 inch (Figure 1) to reduce the simulation time and avoid convergence issues due to such a small grid size. The gridding further away from the fracture (LGR) is coarser as shown in Figure 5.

Water saturation and porosity in the model were obtained from the petrophysical analysis and are shown in Figure 6. Average water saturation is 0.25 and average porosity is 0.07 in the model.

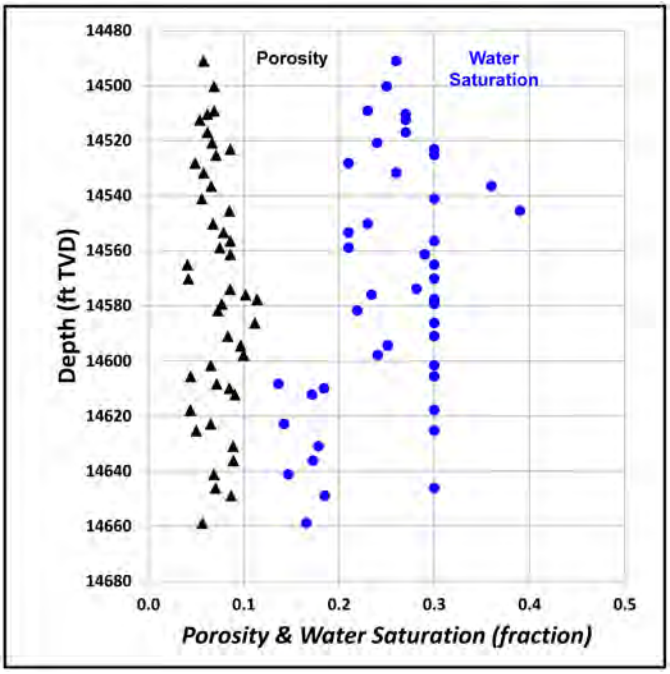

Figure 6—Porosity and water saturation.

Results and Discussion

Initial Well Clean-up and Shut-in

Early time production history-matching results including the fracture clean-up are discussed in this section. History-matching of both water and condensate rates was attempted, with gas production rate as a constraint, by adjusting the following matching parameters: matrix permeability, fracture properties including length and conductivity, non-Darcy factor in the fracture and relative permeabilities. To simulate the water production during the clean-up, we modeled the fracture fluid as water injection prior to the production start-up.

The effective matrix permeability to gas after history-matching is presented in Figure 7. As calculated with the fracture treatment analysis, the matrix permeability is very low ranging from 0.01 to 0.1 mD with a few inter-bedded shales (permeability ≅ 0.1 μD). The overall *kh* in the reservoir is 5.3 mD-ft, resulting in an average initial gas permeability of 0.03 mD. History matched relative permeability curves to all reservoir fluid types (gas-oil-water) in the matrix and in the fracture are shown in Figure 8. Relative permeabilities in the fracture are straight lines, thus there is little pressure loss in the fracture. As the average initial water saturation in the matrix 0.25 is lower than the connate water saturation, there is no mobile water in the matrix unless there is higher water saturation caused by the fracture fluid injection.

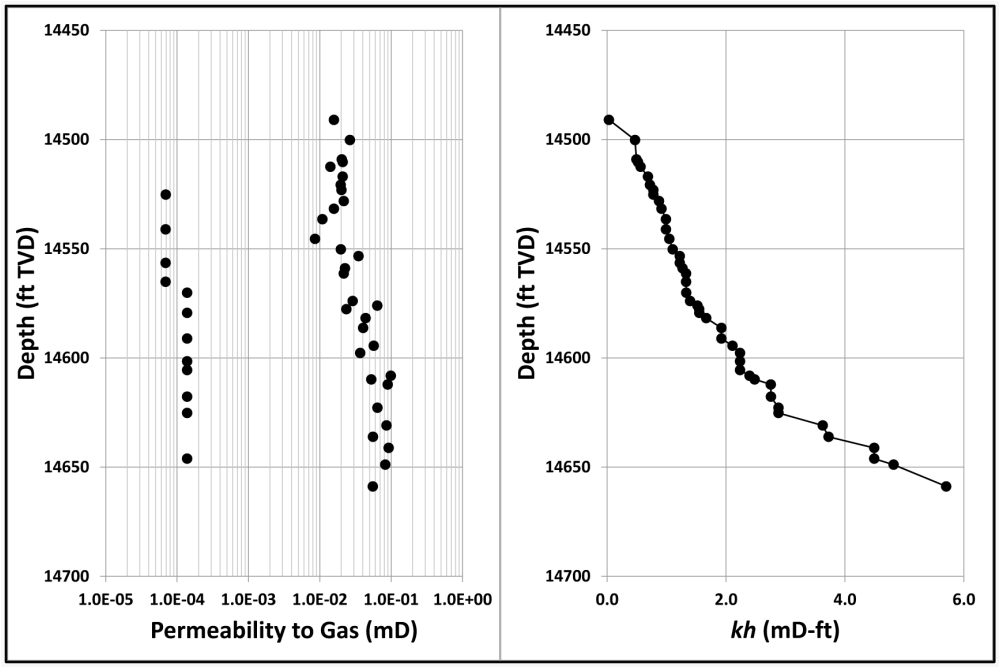

Figure 7—History matching results - initial permeability.

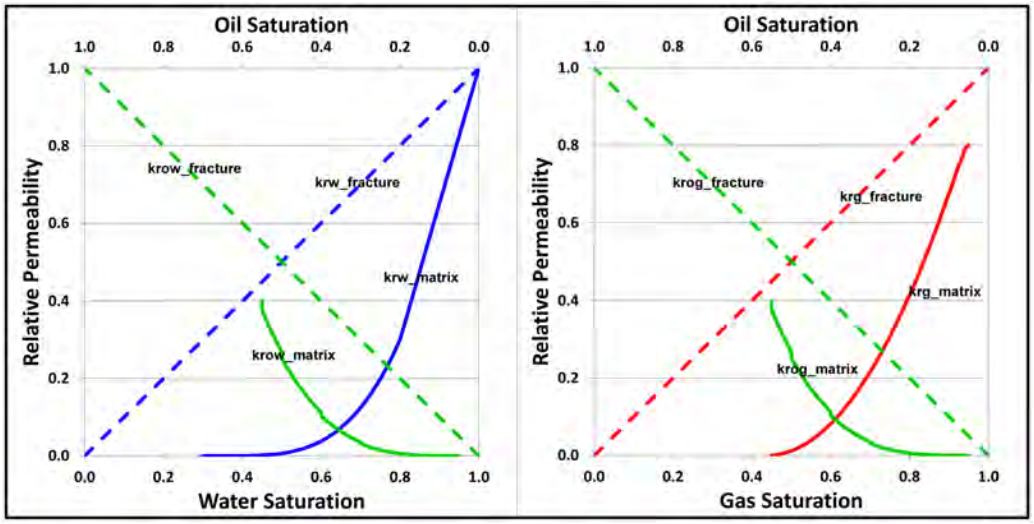

Figure 8—Saturation functions for history matching.

Effective fracture lengths of 800 ft and 600 ft for Stage#1 and Stage#2 have been used in the reservoir simulation model to obtain the best history match. These lengths are 50% of the estimated propped fracture lengths. Seeing an effective propped length of 50% of the created propped length is well within the range of effective propped length in tight gas reservoirs, which is typically 40 to 70% of created propped length. We used the dimensionless fracture conductivities of 0.52 and 1.48 for Stage#1 and Stage#2 respectively, the same as the results from the fracture treatment analysis.

The dependence of permeability on pressure was accounted for by using the *kh* vs. depth given in Figure 9 for both matrix and fracture (Shaoul, et. al., 2015) for both matrix and fracture. For the fracture, the permeability versus pressure is a measured function from laboratory tests for a specific proppant. For the reservoir matrix, effective matrix permeability was one of history matching parameters and the maximum stress sensitive permeability reduction in this study is about 15% compared to the initial permeability.

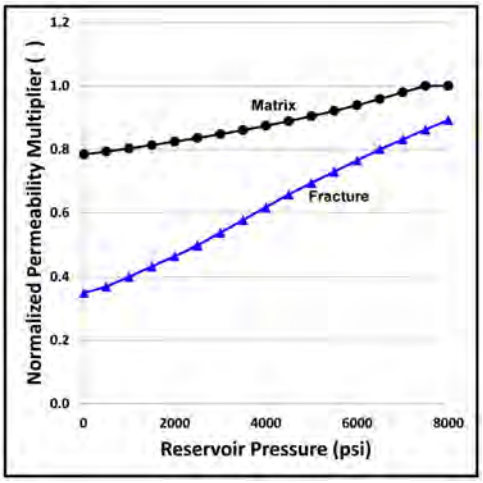

Figure 9—Pressure dependent permeability.

To take into account pressure losses due to poor fracture clean-up, multi-phase effects and convergent flow, we used the non-Darcy factor of 1.0 day/Mscf (D-factor) in all open well connections in the model for the initial clean-up history matching. To be more accurate, this could have been done by setting a lower permeability zone near perforations in the fracture. But this method also requires assumptions about the dimension and degree of fracture damage, and the depressed permeability needs to be increasing as the fracture is cleaning. Instead of simulating the fracture damage zone, we approximate all fracture damage effects and poor clean-up as a skin factor at the well connection, which is in this study, the non-Darcy factor. The above non-Darcy skin factor is rather large, indicating that there is a rather large pressure drop near the perforation in the fracture during the initial clean-up.

History-matching results

History matching results are shown in Figure 10 and Figure 11. The well started production one day after the second stage of fracturing was finished. As shown in the figures, except for the initial peak production, the model shows excellent matching to the historical data, not only for the calculated bottomhole pressure but also for water and condensate rates. At the same time, we observe a decreasing gas rate with decreasing bottom-hole pressure even during the initial stage of production with reservoir pressure higher than 7,000 psi. This behavior can indicate a small drainage volume or, in this case, permeability reduction due to increase effective stress. During the flow period, the water-gas-ratio (WGR) decreased from 15 to 5 STB/MMscf and the condensate-gas-ratio (CGR) was almost constant at nearly 85 STB/MMscf.

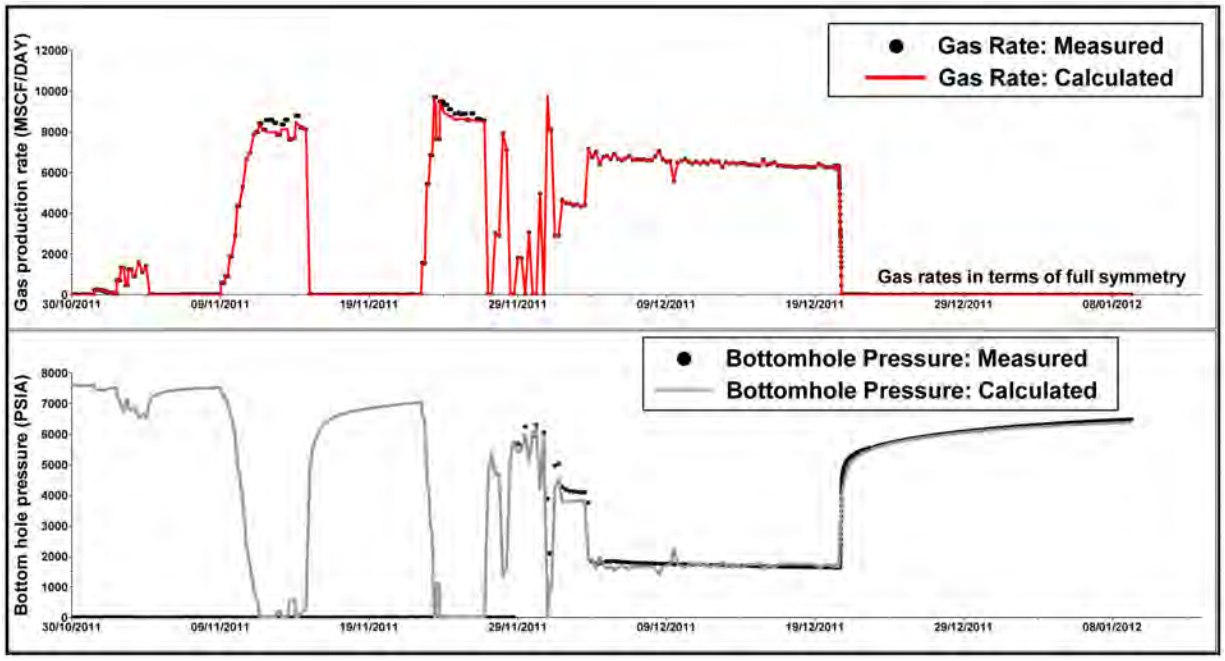

Figure 10—Early time welltest matching results: gas rate constraints and bottomhole pressure.

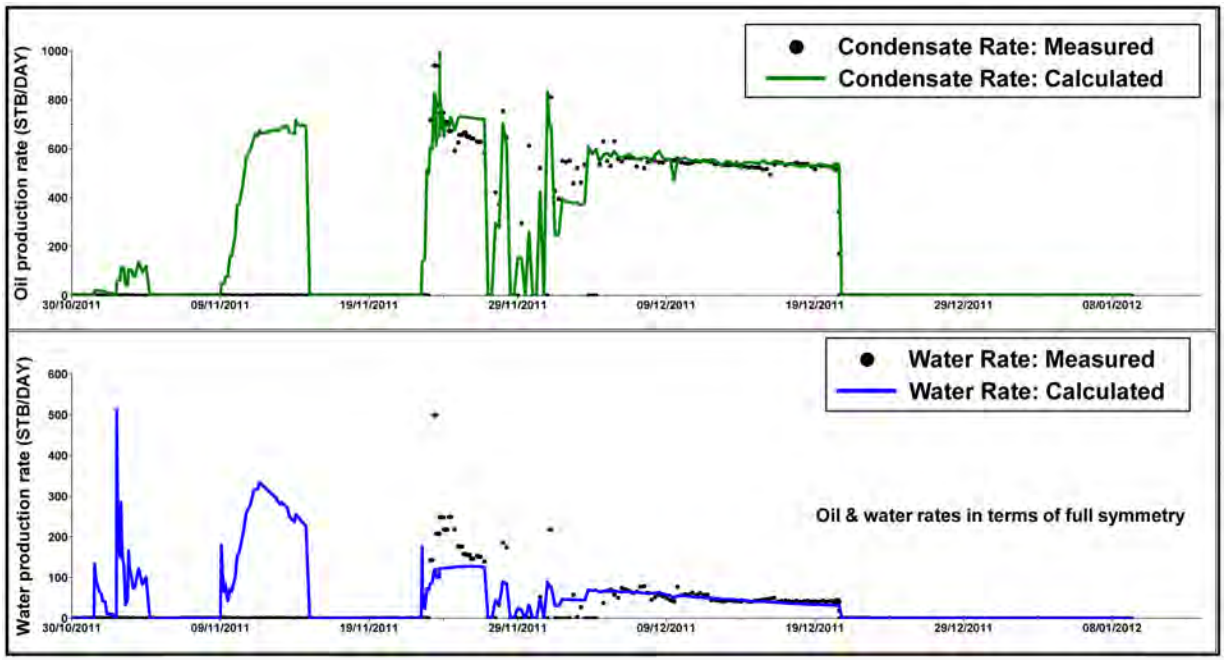

Figure 11—Early time welltest matching results: condensate and water rate.

Pressure distributions in the simulation model at the start of clean-up and by the end of the flow period are shown in Figure 12. As expected, the pressure is much lower in the fracture than in the matrix. Depletion in the tight matrix is only seen in the vicinity of the fracture face at the end of one-month production period. This can be seen in the Figure 13 as well, which shows the pressure drop changes at different grids in the perpendicular direction to fracture (in Y-direction with the same X- and Z-coordinates) from the fracture into matrix by the end of flow period. The pressure drop in the fracture compared to the initial reservoir pressure by the end of flow period reaches 60% of the initial reservoir pressure (Δp = 4,500 psi) after one month of production as shown in the figure. In Figure 14, the pressure drop changes over flow period time at different locations in the longitudinal direction of the fracture (in X-direction with the same Y- and Z-coordinates)

are compared. The largest pressure drop in the fractures occurs immediately outside the perforations (where the velocity is highest) and decreases as the distance from the perforation is increases. Possible explanations to this are: the multi-phase flow effects with water and condensate drop-out and convergent flow effects near the perforations during the initial clean-up.

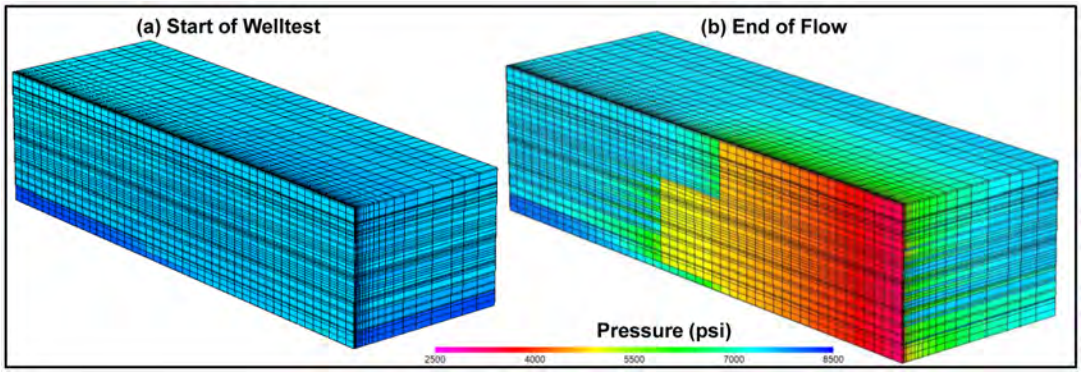

Figure 12—Pressure changes in the model (LGR only).

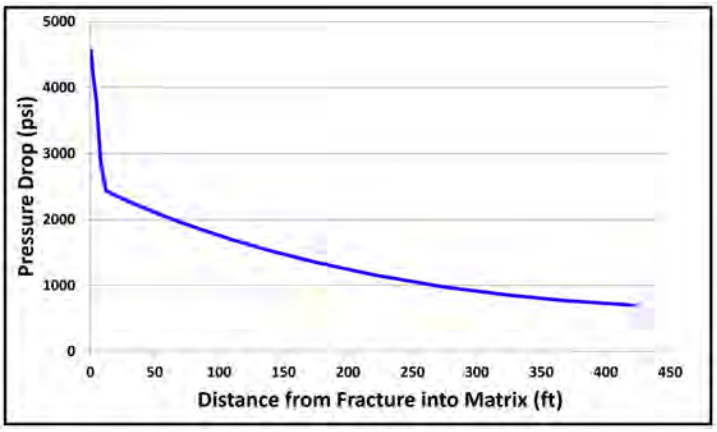

Figure 13—Pressure depletion in the reservoir at increasing distance from fracture plane.

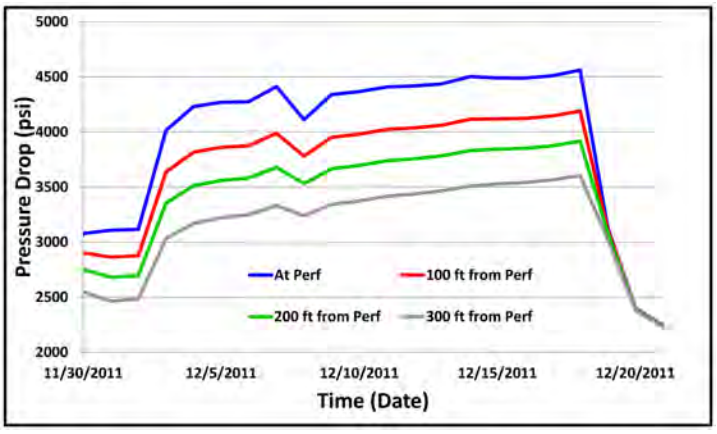

Figure 14—Pressure drop in the fracture during the flow period at different locations from perforation.

The condensate saturation in the simulation model at the end of flow period is shown in Figure 15 comparing oil saturation distributions in the fracture (left) and in the matrix (right). There are a few grid blocks in the fracture with oil saturation of 5-10%. In the matrix, oil saturation is still minimal with maximum values of 2% as the reservoir pressure is about 3,500 psi. At this level of pressure in the matrix, less than

40% of total liquid drop-out occurs (Figure 2). This is insufficient to cause any high oil saturation in the matrix grid which could cause pressure loss during production. Thus, until the end of initial clean-up of 1 month, the major pressure loss is happening only in the fracture and there is no significant condensate banking in the reservoir.

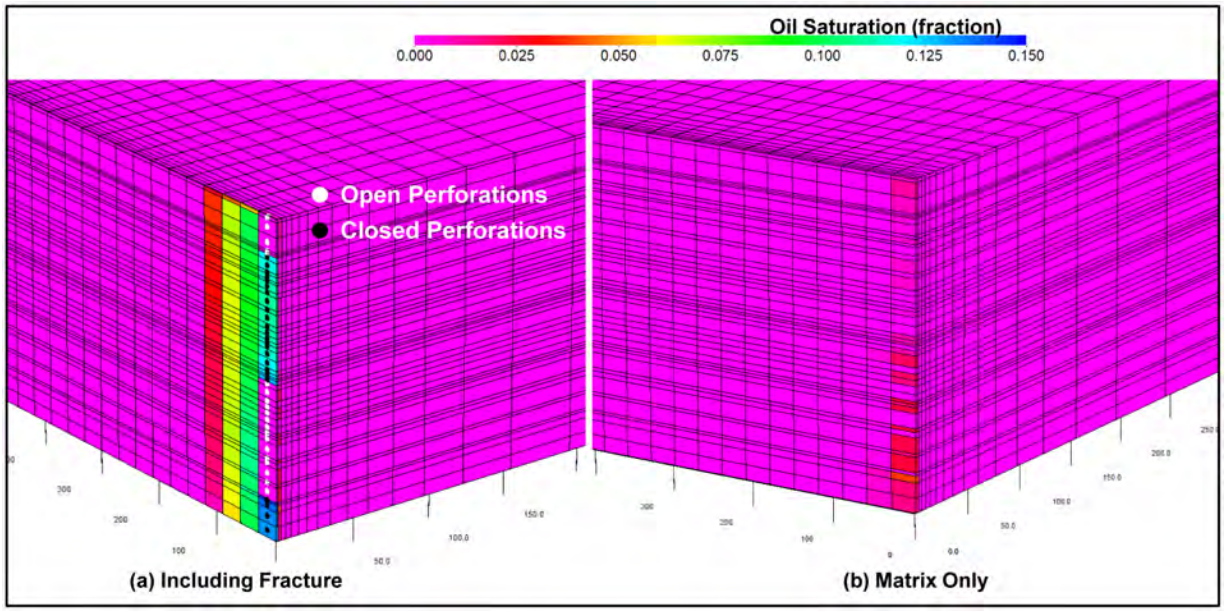

Figure 15—Condensate saturation at the end of the flow period: (a) including fracture and (b) matrix only.

History-Matching Results: Long-Term Production

The long-term production in A-09 well started in January 2015 after 3 years of shut-in. The production data (calculated BHP from measured THP and condensate rate) have been history matched based on a gas rate constraint with the same simulation model used for the initial clean-up matching. Reservoir parameters including matrix permeability, water saturation, porosity and drainage area and fracture parameters are exactly the same as the initial clean-up matching model. Only the non-Darcy factor was varied for this long-term production history-matching. Daily production data including gas rates, condensate rates and calculated bottomhole pressure have been used. Bottomhole pressure has been calculated with a correlation developed in each well using gas rates and wellhead pressure data. Although water rates were not measured in this well, it would be minimal based on field production data.

The long-term production data was history-matched with a lower non-Darcy factor of 0.2 day/Mscf instead of 1.0 day/Mscf which was used for initial clean-up matching. The lower D-factor indicates that the extra pressure losses in the fracture just outside the perforations during the initial clean-up have decreased during the long shut-in possibly due to capillary pressure effects in the tight reservoir, which results in no water production after the 3 year shut-in period. Except for the non-Darcy factor modification, all the other parameters, as mentioned in the previous paragraph, are the same as the model used for initial clean-up matching. History matching results are shown in Figure 16 and Figure 17. With the given gas rates constraints, a good history-matching of the bottomhole pressure and condensate rates was achieved, as shown in the Figure. The trend of CGR, becoming leaner as production goes on, is also matches well with the early and later production timelines. Over the 3 years of production period, the CGR decreased from 85 to 40 STB/MMscf in the well A-09 indicating that condensate dropout has been occurring in the reservoir.

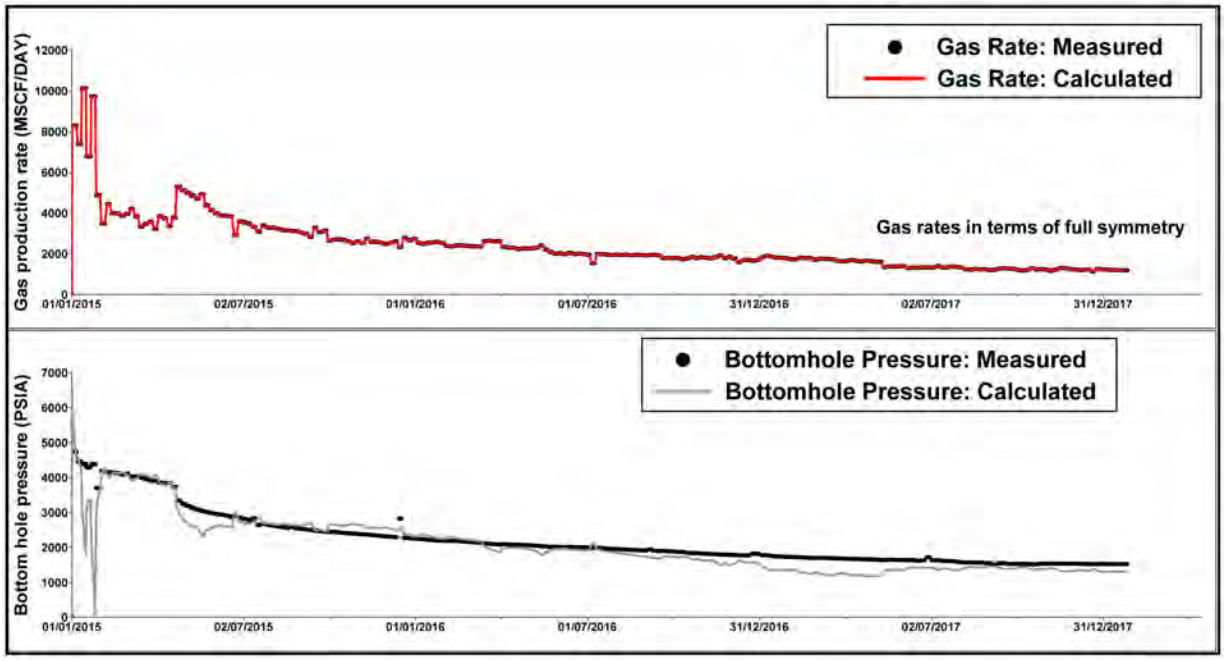

Figure 16—Long term production matching results: gas rate constraints and bottomhole pressure.

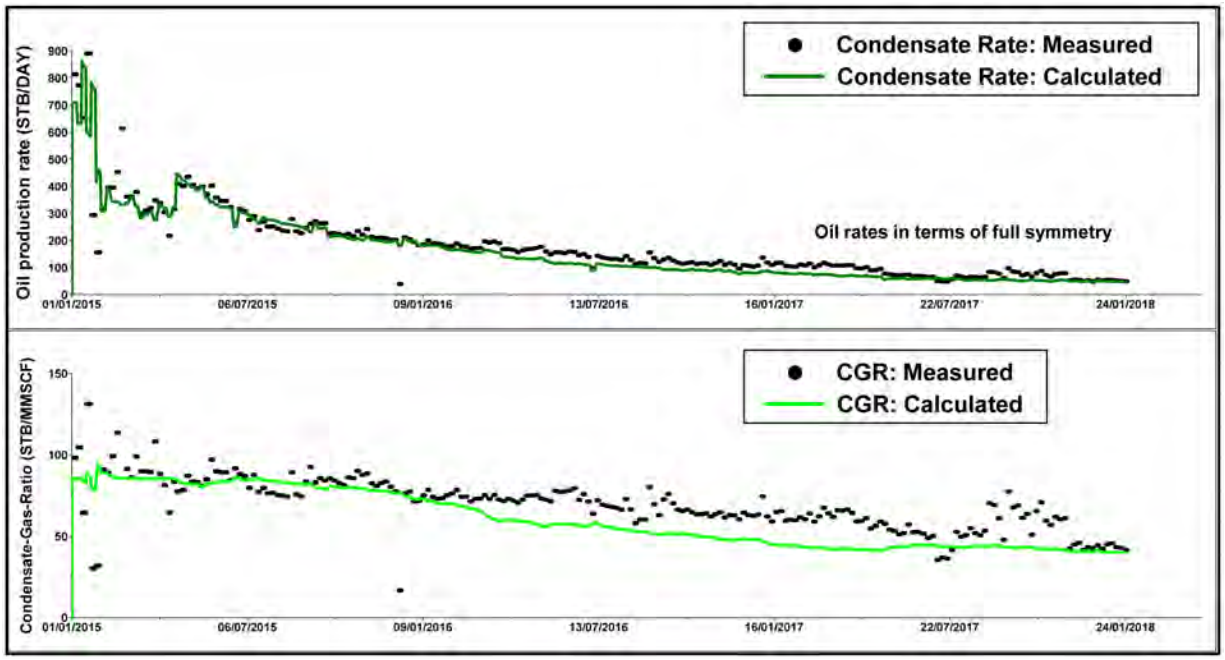

Figure 17—Long term production matching results: condensate rates and condensate-gas-ratio.

Pressure distribution in the simulation model at the end of production is shown in Figure 18. The pressure in the upper layers, with a poorer reservoir quality than the lower layers (Figure 7), is higher than the lower layers by 1,000 psi suggesting that upper layers contribute less to the overall production. Pressure distribution in layers #14 and #41 are compared in Figure 19. These two different layers are selected to represent a low permeability reservoir layer (#14) and a higher permeability reservoir layer (#41) with initial effective gas permeability of 0.01 and 0.09 mD respectively. The degree of depletion in these layers is quite different, not only in the area further away from the fractures but also in the area near the fractures. In the near fracture region, the pressure difference between these two layers is about 2,000 psi, and in the grid blocks further away from the fracture it is about 2,500 psi. This strongly suggests that reservoir permeability

is one of the most important factors determining production performance in tight reservoir, in addition to the properties of the propped fracture.

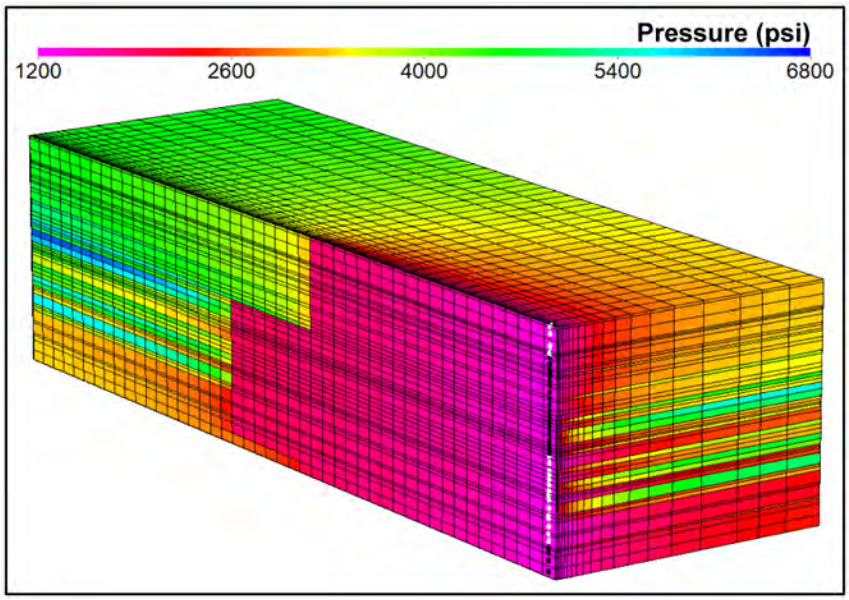

Figure 18—Pressure distribution in the simulation model at the end of production.

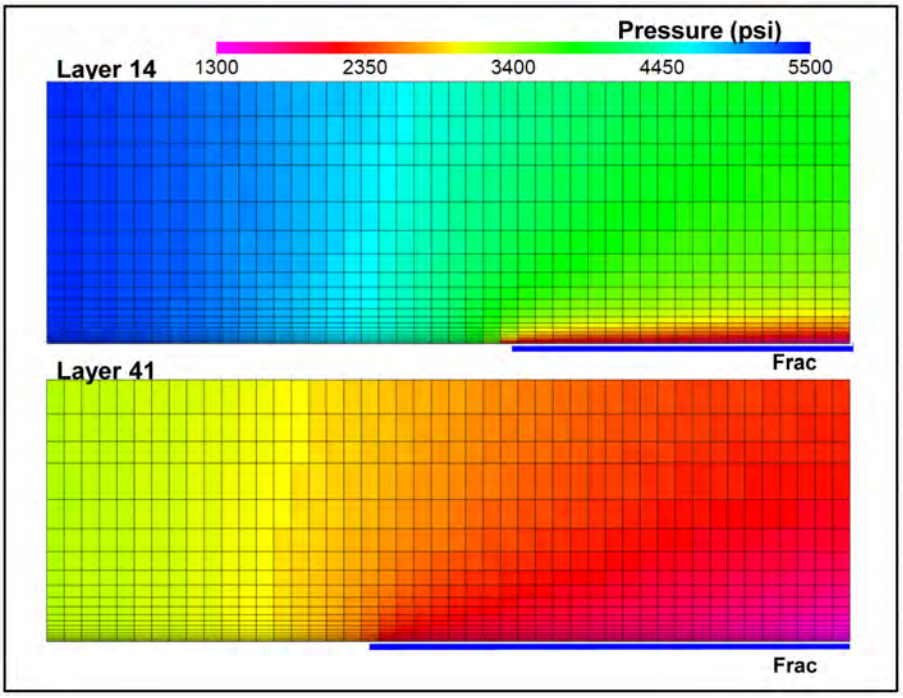

Figure 19—Pressure distribution in layers 14 and 41 at the end of production.

Condensate saturations in the fracture plane and matrix at the end of the long-term production period are shown in Figure 20. Some of condensate accumulates in the bottom part of fracture where its saturation reaches very high values up to 80% due to gravity. However as shown in condensate production, most of condensate was produced through the fracture to surface. Condensate saturation in the fracture plane is very low (less than 1%) except at the very bottom due to the very high effective permeability to oil of the proppant in the fracture. The condensate in the fracture flows towards the perforations with little pressure

loss. The condensate saturation in the fracture is only significant (20-30%) at the very bottom of fracture, where there are no open perforations, and the condensate would have to flow up where the fracture width is the smallest. However, in the matrix it only reaches 20% in the vicinity of the fracture. The condensate distributions in a low permeability reservoir layer (#14) and in a higher permeability reservoir layer (#41) are compared in Figure 21. In the low permeability layer, condensate drops out only in a limited region of matrix close to the fracture face, while in the better reservoir condensate drops out over the entire layer.

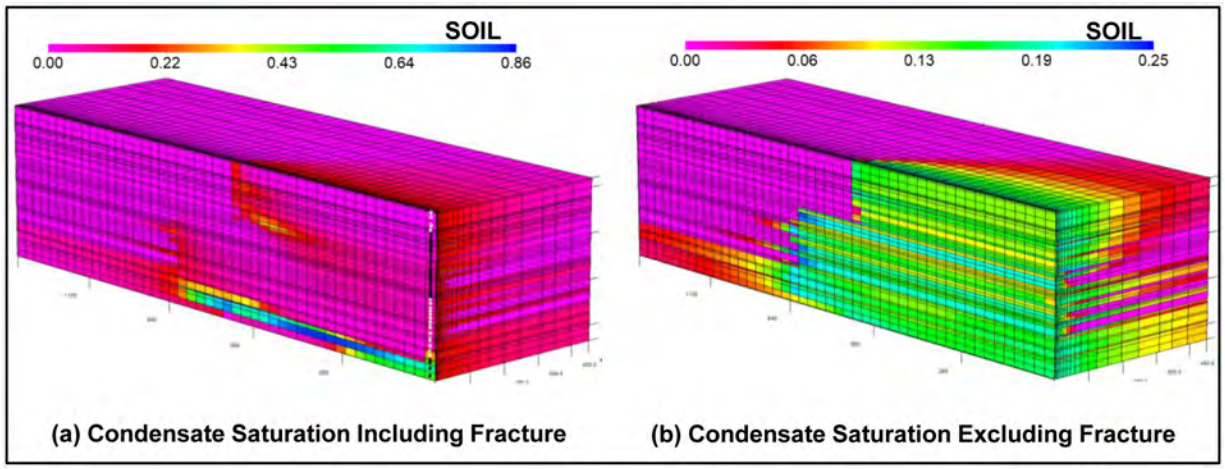

Figure 20—Condensate saturation comparison between fracture (left) and matrix (right).

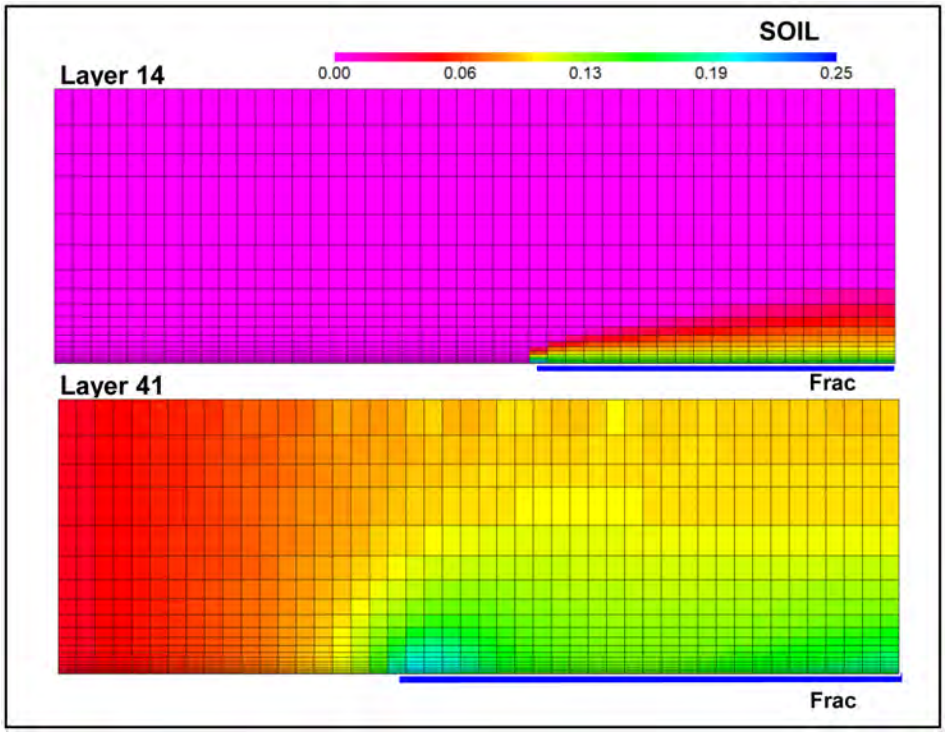

Figure 21—Condensate saturation in layers 14 and 41 at the end of production.

Black Oil vs. Compositional Simulation Models

Black oil simulation models are commonly used to simulate the production from gas condensate reservoirs. This is often done to minimize the time and efforts required to build a more complex compositional model. In this section we compared the history matching of the initial clean-up and the long-term production periods of

well for well A-09 done by this approached with those obtained using a compositional numerical simulator reported above, all things equal otherwise (Alsultan, 2020).

Figure 22 shows the history-matched bottomhole pressure for both black oil and compositional models constrained with gas rates for all cases. Both models agree well for the initial clean-up flow, buildup, and the long-term production data. Both are calibrated with initial clean-up, buildup, and long-term production data. Both models (with the same GIIPs) were run for 20 years to compare the predicted estimated ultimate recovery (EUR) and production profiles.

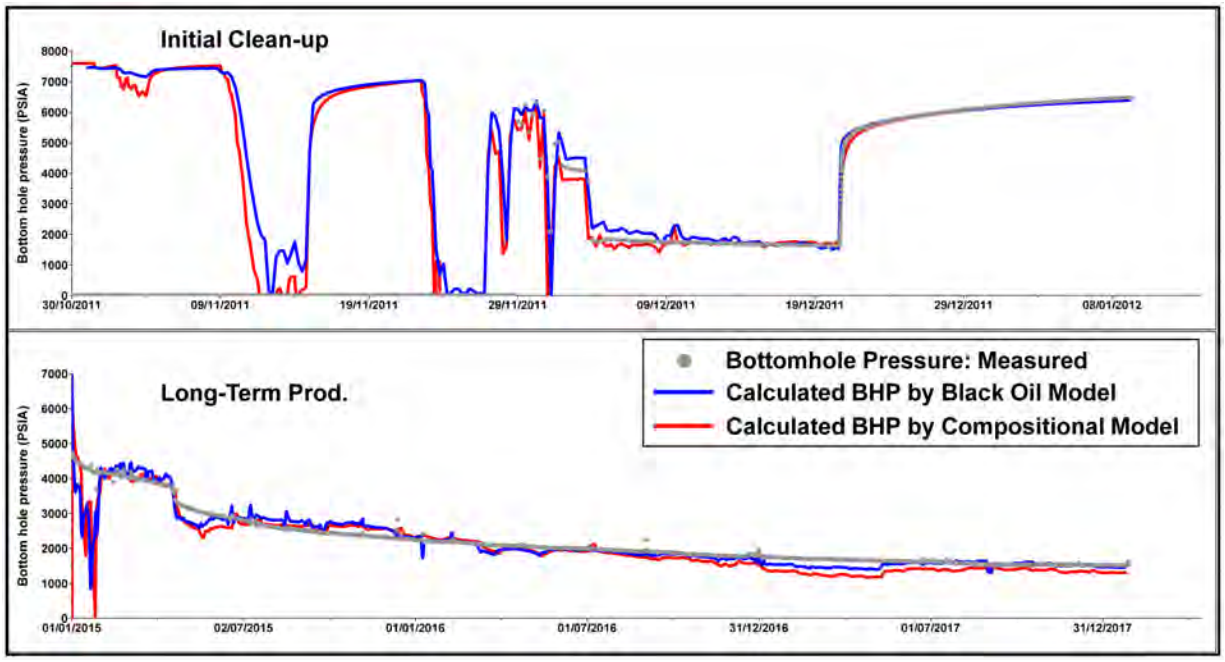

Figure 22—Comparison of history matching results for black oil and compositional models. Long-term BHP is calculated from THP.

The EUR's obtained with both models are shown in Figure 23. The results reveal that gas production predicted by the black oil is systematically higher than that predicted by the compositional model, the difference reaching more than 20% after 20 years.

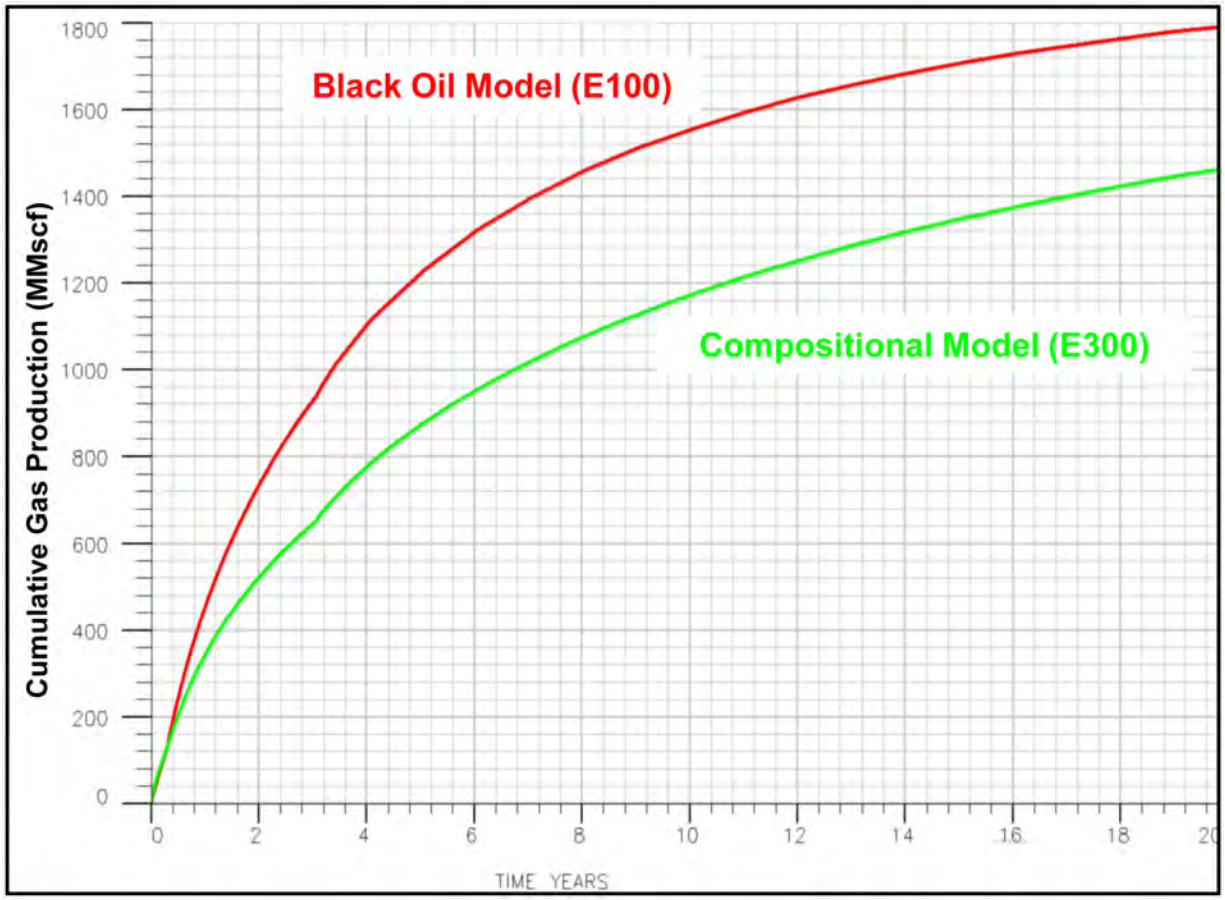

Figure 23—Cumulative gas production (EUR) comparison between black oil and compositional models.

The difference in the model results is caused by the effective permeability reduction in the reservoir due to condensate dropout, which can only be included in a compositional model. The results suggest that to evaluate the hydrocarbon production in an accurate way in a fracture stimulated ultra-tight gas-condensate reservoir, we need a compositional model that has a realistic representation of fracture and reservoir properties (especially relative permeability in the matrix), calibrated with production data. Even if a good history match can be achieved over a period of 2 to 3 years with a black oil model, it does not mean that the black oil model is capturing all the effects that are important over the life of the well, which could be 10 to 20 years.

Conclusions

- Production data history-matching, including gas and liquid rates, has been done in a fracture stimulated unconventional gas-condensate reservoir using a 3-D compositional simulation model. In order to achieve a good history match for both the initial post-fracture clean-up test and the long-term production data, detailed descriptions of fracture & matrix properties and fluid characterization are essential.
- A local grid refinement with high permeability cells was used to represent each stage of the propped fracture in the vertical well in the reservoir model. Fracture dimensions and conductivity were estimated from the fracture treatment data using fracture modeling software which outputs grid information for the numerical reservoir simulator. By using an LGR with a detailed description of the fracture in the simulation model, a more thorough description of condensate flow in the matrix and fracture was possible.

- During the one month of initial clean-up flow, we were able to investigate a minor condensate banking effect in the fracture. Most of the pressure drop is in the fracture and condensate drop-out begins only in the fracture. However, the condensate saturation in the fracture is too small to cause a pressure loss in the fracture. In the matrix, the condensate saturation is almost zero after such a short production period.
- After 3 years of production, the condensate saturation in the fracture is only 1%: the fracture has high permeability with little pressure loss due to multi-phase effects. Most of condensate drop-out appears in the better permeability layers in the reservoir, where condensate saturation reaches up to 20%. In the poor permeability layers, condensate accumulates only in the vicinity of the fracture face. This study suggests that in a hydraulically fractured tight gas-condensate reservoir, pressure loss by condensate banking is occurring in the better quality (but still low permeability) layers and there is little pressure loss in the hydraulic fracture due to condensate.
- It was possible to get a good history match of all the data using both the black oil and the compositional models. But the 20 year estimated ultimate recovery (EUR) is over-estimated by 20% using the black oil model compared to the compositional model. With comparable reservoir and fracture properties in both models, the only difference is condensate dropping out in the compositional model, affecting the relative permeability to gas. In order to evaluate the long-term performance of tight gas-condensate reservoirs, realistic representations of the propped fracture using an LGR, realistic relative permeability curves and high resolution PVT analysis in a compositional model are essential.

References

Al Habsi, G., S. Ghanbarzadeh, S. Motealleh, and B. Al Busafi. "Hydraulic Fracturing: Best Remedy for Condensate Banking Effects in Tight Gas-Condensate Reservoirs." Paper Presented at the Abu Dhabi International Petroleum Exhibition & Conference, Abu Dhabi, UAE, November 2019., https://doi.org/10.2118/197422-MS.

Alakbarov, S., and A. Behr. "Explicit Numerical Evaluation of Productivity Impairment in Hydraulically Fractured Wells of Gas Condensate Reservoirs." Paper Presented at the SPE Russian Petroleum Technology Conference, Virtual, October 2020, https://doi.org/10.2118/201953-MS.

Al-Hashim, H.S., and S.S. Hashmi. "Long-Term Performance of Hydraulically Fractured Layered Rich Gas Condensate Reservoir." Paper Presented at the International Oil and Gas Conference and Exhibition in China, Beijing, China, November 2000.,

Alsultan, Ali. "Effect of Condensate Dropout on Well Productivity in Propped Fracture Stimulated 'Unconventional' Gas/Condensate Reservoirs." TU Delft Master's Thesis. September, 2020.

Barnum, R.S., F.P. Brinkman, T.W. Richardson, and A.G. Spillette. "Gas Condensate Reservoir Behaviour: Productivity and Recovery Reduction Due to Condensation." Paper Presented at the SPE Annual Technical Conference and Exhibition, Dallas, Texas, October 1995., https://doi.org/10.2118/30767-MS.

Crockett, A.R., N.M. Okusu, and M.P. Cleary. "A Complete Integrated Model for Design and Real-Time Analysis of Hydraulic Fracturing Operations." Paper Presented at the SPE California Regional Meeting, Oakland, California, April 1986., https://doi.org/10.2118/15069-MS.

Cronquist, C. "Dimensionless PVT Behavior of Gulf Coast Reservoir Oils." *J. Pet. Technol*. **25**, no. 05 (May 1973): 538. https://doi.org/10.2118/4100-PA.

El-Banbi, Ahmed H., W.D. McCain, Jr., and M.E. Semmelbeck. "Investigation of Well Productivity in Gas-Condensate Reservoirs." Paper Presented at the SPE/CERI Gas Technology Symposium, Calgary, Alberta, Canada, April 2000., https://doi.org/10.2118/59773-MS.

Fevang, O. Gas Condensate Flow Behavior and Sampling. A Dissertation for the Partial Fulfillment of Requirements for the Degree of Doktor Ingenior. Division of Petroleum Engineering and Applied Geophysics, The Norwegian Institute of Technology University of Trondheim, 1995.

Fevang, O., and C.H. Whitson. "Modeling Gas-Condensate Well Deliverability." *SPE Res Eng* **11**, no. 04 (November 1996): 221–30. https://doi.org/10.2118/30714-PA.

Lin, Z.S., and R.J. Finley. "Reservoir Engineering Properties and Production Characteristics of Selected Tight Gas Fields, Travis Peak Formation, East Texas Basin." Paper Presented at the SPE/DOE Low Permeability Gas Reservoirs Symposium, Denver, Colorado, May 1985, https://doi.org/10.2118/13901-MS.

McCain, W.D. The Properties of Petroleum Fluids. PennWell Books, Tulsa, OK, 1990.

Romero, D.J., P.P. Valko, and M.J. Economides. "The Optimization of the Productivity Index and the Fracture Geometry of a Stimulated Well with Fracture Face and Choke Skins." Paper Presented at the International Symposium and Exhibition on Formation Damage Control, Lafayette, Louisiana, February 2002, https://doi.org/10.2118/73758-MS.

Shaoul, Josef, A. Ayush, J. Park, and C.J. de Pater. "The Effect of Stress Sensitive Permeability Reduction on the Evaluation of Post-Fracture Welltests in Tight Gas and Unconventional Reservoirs." The SPE European Formation Damage Conference, 3-5 June 2015, Budapest, Hungary, n.d. http://dx.doi.org/10.2118/174187-MS.

Shaoul, J.R., A. Behr, and G. Mtchedlishvili. "Developing a Tool for 3D Reservoir Simulation of Hydraulically Fractured Wells." *SPE Res Eval & Eng* **10**, no. 01 (February 2007): 50–59. https://doi.org/10.2118/108321-PA.

Shi, C. Flow Behavior of Gas-Condensate Wells. A dissertation submitted to the department of energy resources engineering and the committee on graduate studies of Stanford University in partial fulfillment of the requirements for the degree of doctor of philosophy. Stanford University, 2009.